Physics in SHAPE

1.1 Introduction

The algorithms implemented in SHAPE to simulate radiative transfer are designed to be exceptionally fast and low on memory usage. SHAPE uses a ray-casting algorithm instead of the more popular Monte-Carlo method. Although less accurate, the ray-casting algorithm is orders of magnitude faster than Monte-Carlo and is most suitable to the interactive modeling of SHAPE, allowing for the quick exploration of the potentially vast parameter space involved. The main difference between radiative transfer in SHAPE and typical Monte-Carlo code is that the attributes (such as temperature) at each point in space is *input* and not calculated by the code. In other words, heating is not taken into account. For situations where the final temperature is known (may be a 3D function of position) and one wants to determine the intensity of the light escaping the medium, SHAPE is ideal.

This document outlines in detail the algorithms used in SHAPE to simulate radiative transfer and the approximations used. Where applicable, tests have been conducted indicating the strength of the methods.

1.2 Absorption / Emission

1.2.1 Equations

The amount of radiant energy that passes through the area dA with normal n in a direction with solid angle $d\Omega$ centered about k with a photon frequency between ν and $\nu + d\nu$ in a time dt is:

$$dE = I_\nu k \cdot n \cdot dA \cdot d\Omega \cdot d\nu \cdot dt \tag{1.1}$$

Here I_ν is the specific intensity and has the units of J m^{-2} s^{-1} Hz^{-1} $ster^{-1}$. As light passes through a medium, two things can happen to it:

- Energy is removed from the light (absorption)
- Energy is added to the light (emission)

If the beam travels an infinitesimal distance ds in the k direction, then the amount of intensity added to the beam is:

$$dI_\nu = j_\nu ds \tag{1.2}$$

Where j_ν is the emission coefficient with units of J m^{-3} s^{-1} Hz^{-1} $ster^{-1}$. Similarly the amount of intensity removed from the beam over the distance ds is:

$$dI_\nu = -\kappa_\nu I_\nu ds \tag{1.3}$$

Where κ_ν is the absorption coefficient which has units of m^{-1}. The absorption coefficient is the fraction of intensity that is removed over the interval ds. The total change in intensity over the distance ds is then:

$$\frac{dI_\nu}{ds} = j_\nu - \kappa_\nu I_\nu \tag{1.4}$$

We are interested in what happens to a beam as it passes through an object from an initial point s_0 to a final point s_1. To find the emergent intensity of the beam, we must integrate equation (1.4). To simplify the integration we will define the source function as:

$$S_\nu = \frac{j_\nu}{\kappa_\nu} \tag{1.5}$$

Furthermore, let us define the optical depth as:

$$d\tau_\nu = \kappa_\nu ds \tag{1.6}$$

$$\Rightarrow \tau_\nu = \int_{s_0}^{s_1} \kappa_\nu ds \tag{1.7}$$

Substituting (1.5) and (1.6) into (1.4) gives:

$$\frac{dI_\nu}{d\tau} = S_\nu - I_\nu \tag{1.8}$$

We notice that the derivative:

$$\begin{aligned} &\frac{d}{d\tau}\left[e^{\tau_\nu} I_\nu\right] = e^{\tau_\nu} I_\nu + e^{\tau_\nu} \frac{dI_\nu}{d\tau} \\ &\Rightarrow \frac{dI_\nu}{d\tau} = e^{-\tau_\nu} \frac{d}{d\tau}\left[e^{\tau_\nu} I_\nu\right] - I_\nu \end{aligned} \tag{1.9}$$

We can now substitute (1.9) into (1.8)

$$\begin{aligned} &e^{-\tau_\nu} \frac{d}{d\tau}\left[e^{\tau_\nu} I_\nu\right] - I_\nu = S_\nu - I_\nu \\ &\Rightarrow \frac{d}{d\tau}\left[e^{\tau_\nu} I_\nu\right] = e^{\tau_\nu} S_\nu \end{aligned} \tag{1.10}$$

We can now easily integrate (1.10) to get:

$$\left[e^{\tau_1} I_1 - e^{\tau_0} I_0 \right] = \int_{\tau_0}^{\tau_1} e^{\tau'} S_\nu d\tau' \tag{1.11}$$

The emergent intensity from the medium is where $\tau_0 = 0$. Thus equation (1.11) gives us the intensity that emerges from the object and becomes:

$$I_\nu = e^{-\tau} I_0 + e^{-\tau} \int_0^{\tau} e^{\tau'} S_\nu d\tau' \tag{1.12}$$

We can bring the exponential inside of the integral in the second term giving:

$$I_\nu = e^{-\tau} I_0 + \int_0^{\tau} e^{(\tau' - \tau)} S_\nu d\tau' \tag{1.13}$$

If we now make the substitution:

$$\begin{aligned} t &= \tau - \tau' \\ \Rightarrow dt &= -d\tau' \end{aligned} \tag{1.14}$$

Which when substituted into (1.13) gives:

$$\boxed{I_\nu = e^{-\tau} I_0 + \int_0^{\tau} e^{-t} S_\nu dt} \tag{1.15}$$

1.2.2 Algorithm

1.2.2.1 Grid Creation

The solution to the equation of radiative transfer, equation (1.15), is complicated by the fact that the source function is not constant along ds. If it were, we could easily integrate to get:

$$I_\nu(0) = e^{-\tau_\nu} I_\nu(\tau_\nu) + S_\nu\left(1 - e^{-\tau_\nu}\right) \tag{1.16}$$

In a pure 3D environment solving equation (1.15) analytically or even numerically would be tedious at best. The approach taken by SHAPE is to subdivide all of space into a n^3 grid. Each cell in the grid then contains homogenous attributes such as density, temperature and of course emission and absorption coefficients. Since the source function across a single cell is constant, we can use (1.16) to determine the emergent intensity from that cell. Performing the radiative transfer across each cell in this manner therefore allows us to determine the emergent intensity from our scene. Of course this solution will only be an approximation due to the finite size of the grid cells. A better approximation can be obtained by decreasing the size of each cell in the grid (i.e. increasing the number of cells).

The first step is to create the grid. This step requires determining where in the grid each component of the model should be placed. The approach adopted by SHAPE is to use the mesh outline of the component to determine which cells are occupied by an object. Determining which cells a mesh belongs to is, however, not a simple task.

To accomplish this, we must determine which cells are within the volume (interior) of the mesh. SHAPE does this by casting rays into the mesh and recording where intersections occur. The algorithm then fills in the cells between each pair of intersections. However, some cells will be partially inside and outside of the mesh volume. This problem needs to be addressed otherwise undesirable aliasing effects will be introduced into the final image. In order to circumvent this, the algorithm measures what fraction of each cell is within the mesh and the cell is then "weighted" by this value. This is done by throwing points randomly in the cell and recording the fraction that lie inside the mesh.

It should be noted that if two objects happen to occupy the same cell, each is added to the cell. When the radiative transfer calculations are performed, they are done so for each object in the cell. This adds a slight inaccuracy to the solution, but is deemed acceptable for the simplicity it adds.

1.2.2.2 Ray Casting

The ray-casting algorithm, as the name suggests, casts beams of light throughout the grid. As the beam propogate through the grid, each cell absorbs or emits into it. When the beams emerge from the grid towards the observer, a pixel is rendered on the final image. A beam is a composite of n spectral bands over a wavelength range from $\lambda_{\min}$ to $\lambda_{\max}$.

The distances to the objects under study are not always known. Consequently the solid angle the cells emit into is ill-defined. For this reason it is desirable to find the energy per solid angle and the user can then calculate the energy at the detector if they know the distance. The beams of energy cast through the SHAPE grid are therefore in units of energy per solid angle. Of course this introduces some inaccuracy because each cell will not emit into the same solid angle. However, in SHAPE we assume the distance to the object is so large that all the cells in the grid can be considered at the same distance and the solid angle each cell emits into is indeed the same.

For each x/y column in the grid an initially empty beam of energy (per solid angle) is created just beyond the last cell. This beam is then transferred along the z direction of the grid and the radiative transfer is performed over each cell.

The quantity we are interested in is not the specific intensity, I_ν, but the emergent energy E_ν (per solid angle). The equation of transfer then takes on the form:

$$\begin{aligned} &\frac{dE_\nu}{ds} = j_\nu \cdot A - \kappa_\nu E_\nu \\ &\Rightarrow \frac{dE_\nu}{\kappa_\nu ds} = S_\nu \cdot A - E_\nu \end{aligned} \tag{1.17}$$

Where A is the area of the emitting surface, in our case the surface area of a cell. We are concerned with transfer across a single cell where the source function is held constant. Under this simplification, the solution of (1.17) is:

$$E_\nu = e^{-\tau_\nu} E_0 + S_\nu \cdot A\left(1 - e^{-\tau_\nu}\right) \tag{1.18}$$

Where, if we let Δs represent the cell depth:

$$\tau_\nu = -\kappa_\nu \Delta s \tag{1.19}$$

The beams in SHAPE consist of bands of finite width, $\Delta\nu$. The total energy contained within a single band is therefore:

$$E_{\Delta\nu} = e^{-\tau_\nu} E_0 + S_\nu \cdot A \cdot \Delta\nu\left(1 - e^{-\tau_\nu}\right) \tag{1.20}$$

Where S_ν and τ_ν represent the source function and optical depth respectively at the central frequency of the band.

Equation (1.20) is used by SHAPE to calculate the emergent energy per band over a cell during the ray casting procedure (Figure 0-1). Once the ray has passed through all cells in an x/y column, the resulting energy is converted to a pixel value on the final image.

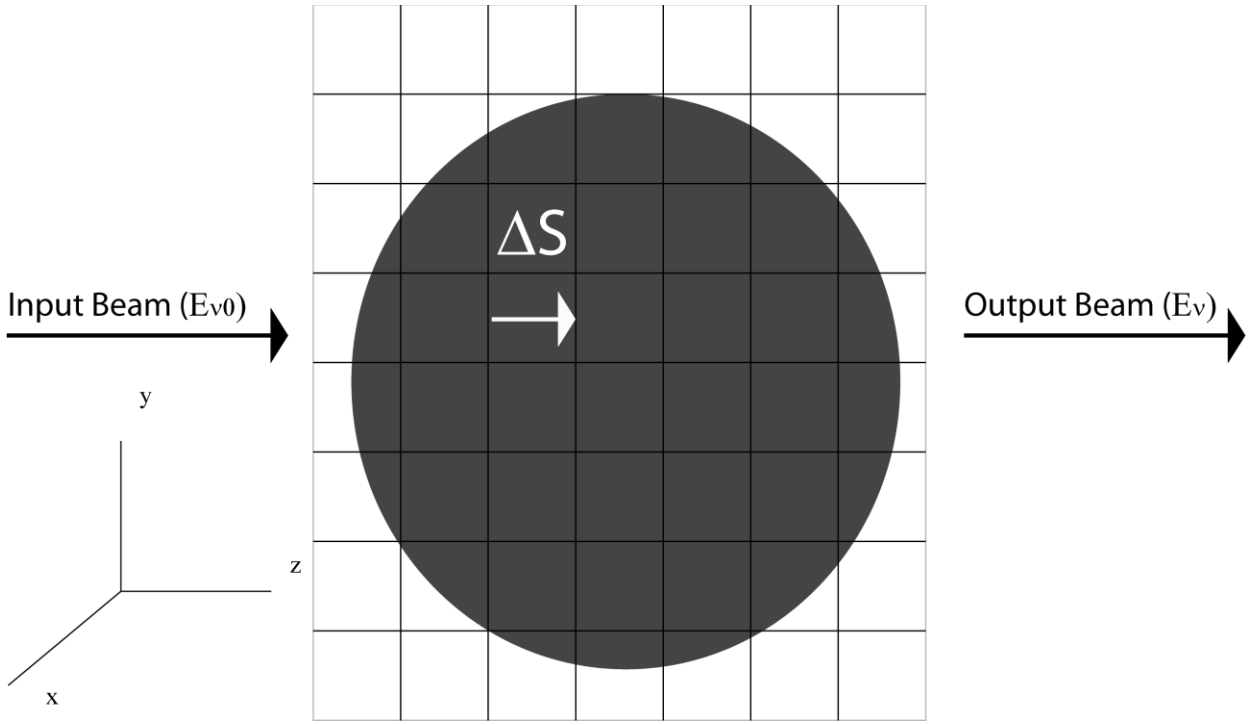

Figure 0-1: Illustration of a volume sphere mapped to the grid. The input beam for each x/y column is initially empty. The transfer in equation (1.20) is performed along each occupied cell for each band in the beam.

1.2.3 SHAPE Accuracy

In order to test the accuracy of the radiative transfer algorithm, I have created a simple SHAPE model that can easily be compared with theory. The model consists of a cube of constant density

of $n = 1\ \mathrm{m}^{-3}$ and dimensions of $5\ \mathrm{pc} \times 5\ \mathrm{pc} \times 5\ \mathrm{pc}$. It is rendered in SHAPE over the wavelengths $4 \times 10^{-7}\ \mathrm{m}$ - $7 \times 10^{-7}\ \mathrm{m}$ using 100 spectral bands. The emission coefficient is :

$$j_\nu = 10^{-15}\ \left(\mathrm{W\ m^3\ ster^{-1}}\right) \cdot n^2 \tag{1.21}$$

and the absorption coefficient is :

$$\kappa_\nu = 10^{-17}\ \mathrm{m^2} \cdot n \tag{1.22}$$

Resulting in the source function:

$$S_\nu = \frac{j_\nu}{\kappa_\nu} = \left(\mathrm{W\ m\ ster^{-1}}\right) \cdot n \tag{1.23}$$

Since the source function is constant, we can use (1.16) directly in order to calculate the theoretical emergent intensity:

$$I_\nu(0) = e^{-\tau_\nu} I_\nu(\tau_\nu) + S_\nu\left(1 - e^{-\tau_\nu}\right) \tag{1.24}$$

Using our model values, we have:

$$\tau_\nu = \kappa_\nu \Delta s = \kappa_\nu \cdot 5\mathrm{pc} \simeq 1.5428 \tag{1.25}$$

$$S_\nu = 100\ \mathrm{W\ m\ ster^{-1}} \tag{1.26}$$

Since there is no initial intensity ($I_\nu(\tau_\nu) = 0$) equation (1.24) yields:

$$I_\nu(0) = 78.6227\ \mathrm{W\ m^{-2}\ Hz^{-1}\ ster^{-1}} \tag{1.27}$$

To get the total luminosity, we have to multiply (1.27) by the area of the face of the cube ($5\ \mathrm{pc}\ \times\ 5\ \mathrm{pc}$), the bandwidth ($d\nu \simeq 3.212 \times 10^{14}\ \mathrm{Hz}$) and 4π ster to get:

$$\boxed{L = 7.5541 \times 10^{51}\ \mathrm{W}} \tag{1.28}$$

The same parameters when run in SHAPE on a 128^3 grid give a luminosity of:

$$\boxed{L_{\text{SHAPE}} = 7.5541 \times 10^{51}\ \text{W}} \tag{1.29}$$

The theoretical and SHAPE values are identical.

1.3 Scattering

Scattering of a photon causes it to move in a new direction with possibly a new frequency. The difficulty in treating scattering in a radiative transfer framework is that the incoming beam can come from any direction, and be scattered into any other direction (for isotropic scattering). Keeping track of all the scattered beams quickly becomes computationally and memory intensive. What is worse is that most of the beams that are tracked will not leave the scene towards the camera. This is a waste of computer resources.

To simplify things, SHAPE only acknowledges single scattering from predefined sources (stars). Therefore the incoming beam is from a known direction and the scattered beam is towards the camera.

When we calculate the radiative transfer as before, there will be an extra absorption (light being scattered *from* the incoming beam) and emission (scattered light from the source beam *into* the incoming beam). The equation of transfer now becomes:

$$\frac{dE_\nu}{ds} = j_\nu \cdot A + \kappa_\nu^s \Phi_\nu - \left(\kappa_\nu^s + \kappa_\nu^a\right) E_\nu \tag{1.30}$$

Where we have divided the absorption coefficients into the scattering absorption coefficient, κ_ν^s, and the absorption coefficient, κ_ν^a. Φ_ν is the energy being scattered into our beam from all directions per solid angle.

$$\Phi_\nu = \oint \phi_\nu\left(\theta'\right) E_\nu\left(\hat{k}'\right) d\Omega' \tag{1.31}$$

The phase function, $\phi_\nu(\theta)$, is the probability of the beam being scattered from the $\hat{k}'$ direction into the $\hat{k}$ direction (θ is the angle between $\hat{k}'$ and $\hat{k}$) into the new solid angle $d\omega$. It is normalized such that:

$$\frac{1}{4\pi}\int \phi_\nu(\theta)\, d\omega = 1 \tag{1.32}$$

As mentioned, in SHAPE we are concerned with single scattering from predefined sources. So we are aware of all the incoming beams. Assuming there are $n+1$ incoming beams to the cell in question we have:

$$\Phi_\nu = \sum_{i=0}^{n} \phi_\nu\left(\theta^i\right) E_\nu\left(\hat{k}^i\right) \tag{1.33}$$

However, there is one beam that can be removed from this sum, namely our input beam in the $\hat{k}$ direction. This gives us:

$$\Phi_\nu = \phi_\nu(0)\, E_\nu\left(\hat{k}\right) + \sum_{i=1}^{n} \phi_\nu\left(\theta^i\right) E_\nu\left(\hat{k}^i\right) \tag{1.34}$$

The sum is now over all inbound beams from the sources. For these beams, the solid angle is known and we can calculate the total energy hitting our cell, $\bar{E}_\nu$. The energy available per solid angle to be reemitted is then $\bar{E}_\nu / 4\pi$ giving us:

$$\Phi_\nu = \phi_\nu(0)\, E_\nu\left(\hat{k}\right) + \frac{1}{4\pi}\sum_{i=1}^{n} \phi_\nu\left(\theta^i\right) \bar{E}_\nu\left(\hat{k}^i\right) \tag{1.35}$$

If we further define:

$$\beta = \frac{1}{4\pi}\sum_{i=1}^{n} \phi_\nu\left(\theta^i\right) \bar{E}_\nu\left(\hat{k}^i\right) \tag{1.36}$$

We have:

$$\Phi_\nu = \phi_\nu(0) E_\nu\left(\hat{k}\right) + \beta \tag{1.37}$$

Substituting (1.37) back into (1.30) gives us:

$$\frac{dE_\nu}{ds} = j_\nu A + \kappa_\nu^s\left(\phi_\nu(0) E_\nu\left(\hat{k}\right) + \beta\right) - \left(\kappa_\nu^s + \kappa_\nu^a\right) E_\nu \tag{1.38}$$

Let us now define:

$$\begin{aligned} j_\nu^{'} &= \left(j_\nu \cdot A + \kappa_\nu^s \beta\right) \\ \kappa_\nu^{'} &= \left(\kappa_\nu^s + \kappa_\nu^a - \phi_\nu(0)\kappa_\nu^s\right) \\ S_\nu^{'} &= \frac{j_\nu^{'}}{\kappa_\nu^{'}} \end{aligned} \tag{1.39}$$

We then have:

$$\begin{aligned} &\frac{dE_\nu}{ds} = j_\nu^{'} - E_\nu \kappa_\nu^{'} \\ &\Rightarrow \frac{dE_\nu}{\kappa_\nu^{'} ds} = S_\nu^{'} - E_\nu \end{aligned} \tag{1.40}$$

Equation (1.40) is in the same form as equation (1.8) which we know the solution to:

$$E_\nu(0) = e^{-\tau_\nu^{'}} E_\nu + \int_0^{\tau_\nu^{'}} S_\nu^{'} e^{-t} dt \tag{1.41}$$

Where we have also made the substitution $\tau_\nu^{'} = -\int_{s_0}^{s_1} \kappa_\nu^{'} ds$. Over the distance of one cell the new source function is also constant leaving us with the solution:

$$E_\nu = e^{-\kappa_\nu^{'}\Delta s} E_0 + S_\nu^{'}\left(1 - e^{-\kappa_\nu^{'}\Delta s}\right) \tag{1.42}$$

Over a band of finite width, this becomes:

$$E_{\Delta\nu} = \left[e^{-\kappa_\nu' \Delta s} E_0 + S_\nu' \left(1 - e^{-\kappa_\nu' \Delta s} \right) \right] \Delta\nu \tag{1.43}$$

Equation (1.43) is what is used in SHAPE to calculate the emerging energy per solid angle from a cell when scattering is involved. The calculation proceeds as before. We create a beam for each x/y column and transfer this beam through all the cells in the z direction. The only difference now is that we need to calculate β for each cell. This involves calculating all of the beams originating at the sources, and ending at the cell in question. A beam is emitted from the source and is transferred (as before) through all the intersecting cells. In this way the beam is absorbed as it travels from the source to the cell. The only difference between this scenario and the x/y column integration is that the path length, Δs, varies from cell to cell instead of just being the cell depth. Once this integration is complete, the resulting beam is added to the current cell and used as a source beam in the calculation of β.

The emitted beam is calculated using the Planck function and the temperature of the source. The Planck function gives the intensity of the beam emitted from the star. However we need the total energy towards the cell, $\bar{E}_\nu$, so we must multiply the intensity by an area and solid angle. The solid angle is the three dimensional angle the cell subtends as seen from the source. To calculate it we simply take the fraction of the surface area of a sphere at distance r (distance from cell to source) that the cell occupies and multiply that by 4π . The entire surface area of a sphere with radius r is $A_T = 4\pi r^2$. To find the area the cell occupies we will use a circle of radius $d/2$ where d is the diagonal of the cell. The area the cell occupies is thus $A_C = \pi \left(d/2 \right)^2$. The solid angle the cell subtends is then:

$$\frac{A_C}{A_T} = \frac{\pi\left(d/2\right)^2}{4\pi r^2} \tag{1.44}$$

$$\Rightarrow \Omega = \frac{\pi d^2}{4r^2} \tag{1.45}$$

The surface area of the emitter (star) is simply $4\pi R^2$, where R is the radius of the star. Multiplying the intensity from the Planck function by the stellar surface area and then by the solid angle, we get the total energy of the beam directed towards the cell. The geometry is depicted in Figure 0-2.

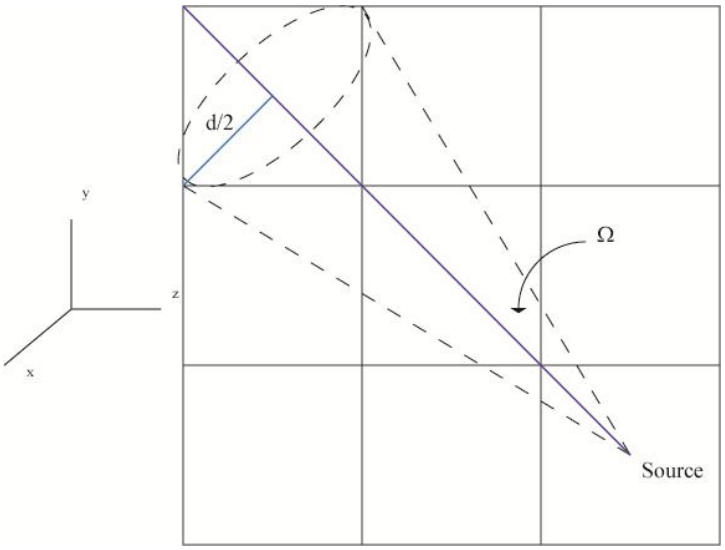

Figure 0-2: Illustration of the source beam calculation. A beam from the source is emitted towards the cell. The beam intensity is multiplied by the solid angle to get units of Joules. Each cell between the source and the cell in question absorbs and emits into the beam.

The total energy absorbed by the cell due to scattering is then:

$$d\bar{E} = \kappa_\nu^s \bar{E}_\nu \tag{1.46}$$

The energy available by the cell to emit per solid angle is therefore:

$$dE = \frac{\kappa_\nu^s \bar{E}_\nu}{4\pi} \tag{1.47}$$

In summary, an input beam is emitted from behind each x/y column in the grid. At each cell along the column, a beam from the source to the cell is emitted and a fraction is added to the input beam (due to scattering). The emergent beam is added to the final image as a pixel value.

To qualitatively demonstrate the effects of scattering in SHAPE, I have created a simple model consisting of a central star ($T_* = 5780$ K, $L_* = L_\odot$) behind a slab of scattering material with constant density. The slab is thicker at the bottom than the top, creating a gradient between the amount of material between the observer and the star (simulating, perhaps, the atmosphere at sunset/sunrise). The absorption and scattering coefficients are $\kappa_\nu^a \propto \lambda^{-1}$ and $\kappa_\nu^s \propto \lambda^{-4}$ respectively. The mesh SHAPE model along with the rendered result is displayed in Figure 0-3. Due to the dependency of the scattering coefficient on the wavelength of the light, the thinner (top) regions are bluer than the thicker bottom regions. The λ^{-1} form of the absorption coefficient adds to the reddening in the thicker regions. The scene was rendered using a 256^3 grid on an Intel(R) Core(TM) i5 processor with 6 GB RAM (1.5 useable for SHAPE) in $t = 11$ s.

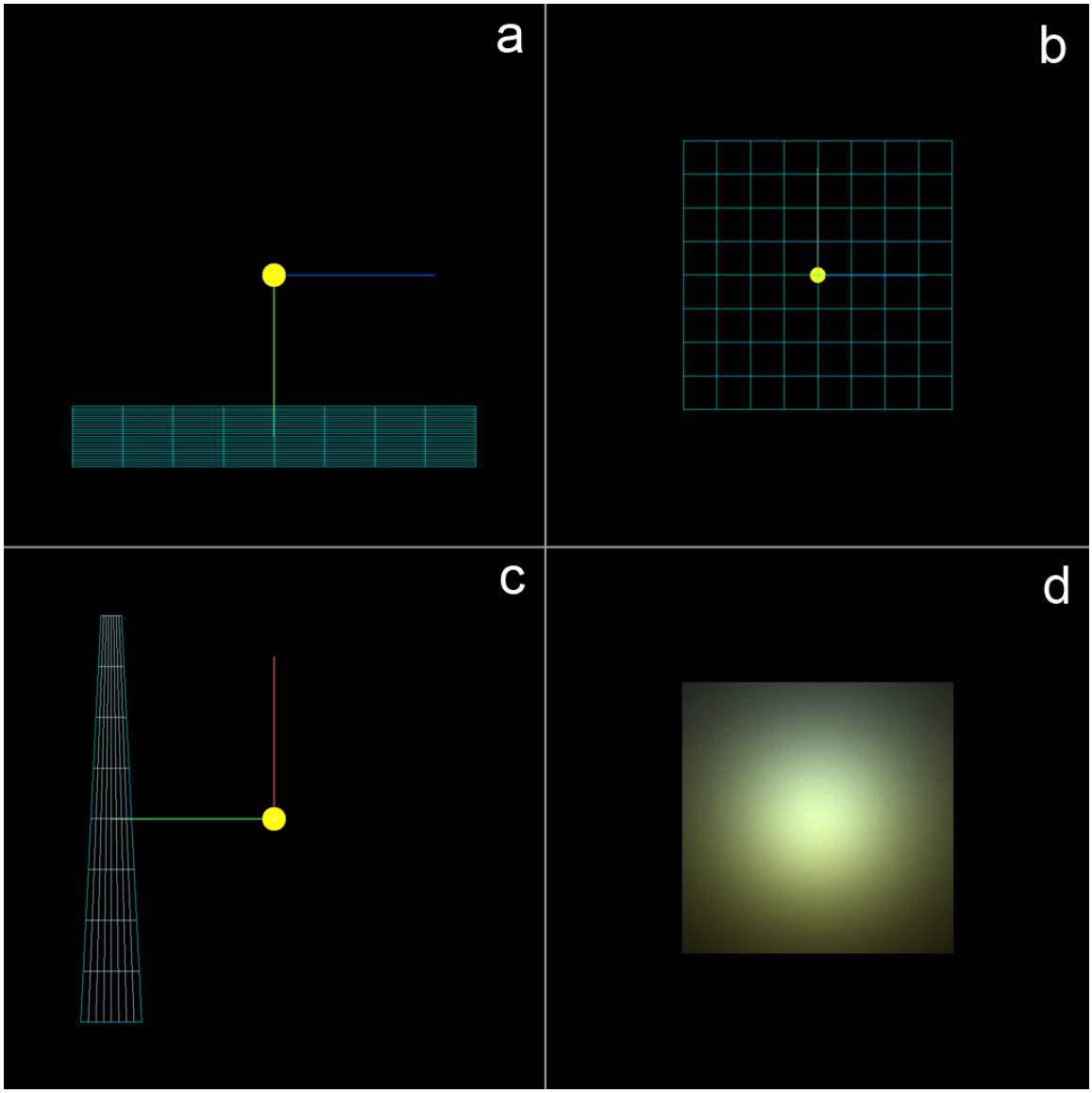

Figure 0-3: SHAPE mesh (panels a,b,c) and SHAPE result (panel d) of a test scattering model. Each mesh panel represents the model from a different direction in order to bettter show it's construction. a) Mesh model from above, b) from the front, c) from the right, d) rendered image.

1.4 Multiple Scattering

In the above algorithm the beam from the source is scattered once towards the camera for each cell. This is a single scattering algorithm. In reality, however, the situation is much more complex as scattering occurs numerous times in all directions. Treating this multiple scattering in a complete way is extremely time-consuming.

The multiple scattering algorithm implemented by SHAPE approximates the process by estimating the total amount of energy scattered *into* each cell by every other cell. The energy a cell has available for scattering to other cells is stored, and after a user defined number of iterations is finally scattered towards the camera. The detailed algorithm is defined below:

1) Calculate the energy reaching each cell, c_0, from the source.
    a) Emit a beam from the source to c_0, performing radiative transfer along each intersecting cell (c_i).
    b) Store the energy of the beam in a secondary 3D array (a_s). This will be the energy available to c_0 for the next iteration in the scattering process.
2) Perform m scattering iterations. Each iteration determines to a higher order the energy scattered towards c_0.
    a) For each cell, c_0, cast n beams from random points on the edge of the grid towards the center of c_0.
    b) Perform radiative transfer through each cell encountered, c_i. Each cell, c_i, will scatter into the beam from their "reserve" ($a_s[i]$).

c) Add the total beam energy to the "reserve" of c_0 for the next iteration ($a_s[0] = a_s[0] + E$)

3) Cast one beam for each x/y column from behind the grid and transfer along each cell using the a_s array as the source of scattering for the algorithm. The resulting beam intensity is converted to a pixel value of the final image.

In the single scattering algorithm, only the 1st and 3rd steps are performed. The inclusion of the second step alters the energy available for scattering from being that solely of the source, to that from a random sampling of other cells. The more beams that are cast towards each cell (n), the better the approximation of the amount of energy scattered into each cell becomes ($n = 1$ assumes equal intensity emission from all directions). For highly asymmetric nebulae, it becomes important for n to be large in order to get a sample from all regions. For nebulae with little structure, fewer beams are adequate. The beams cast through the grid are normalized to 4π steradians and therefore adding more beams will not increase the total energy of the nebula, but simply sample more of it. The radiation field is then set up for a single step. More iterations of this algorithm (m) will lead to a more accurate solution.

It should be noted that this algorithm does not preserve information about the direction of the scattered beams towards each cell. Only the energy of the beam is added to the "reserve" of the cell in question. Therefore, non-isotropic scattering will be handled incorrectly since there is no way to determine the relative angle of the beams. The multiple scattering algorithm presented here is thus valid only for isotropic scattering.

Using the same test model as in the previous section, Figure 0-4 represents several images displaying the effects of multiple scattering. The simulation used the values of $n = 10$ and $m = 4$. Each panel in the figure was created at different iterations (m) of the algorithm. The final result (Figure 0-5) represents the combination of each iteration into a single image. Figure 0-4 demonstrates the effects of higher order scattering; a decrease in energy, a shift towards shorter wavelengths and a diffusion of emission throughout the medium. The addition of these higher order multiple scatterings has little effect on the qualitative appearance of the overall model (Figure 0-5). The scene was rendered using a 128^3 grid on an Intel(R) Core(TM) i5 processor with 6 GB RAM (1.5 useable for SHAPE) in $t = 4.6$ minutes.

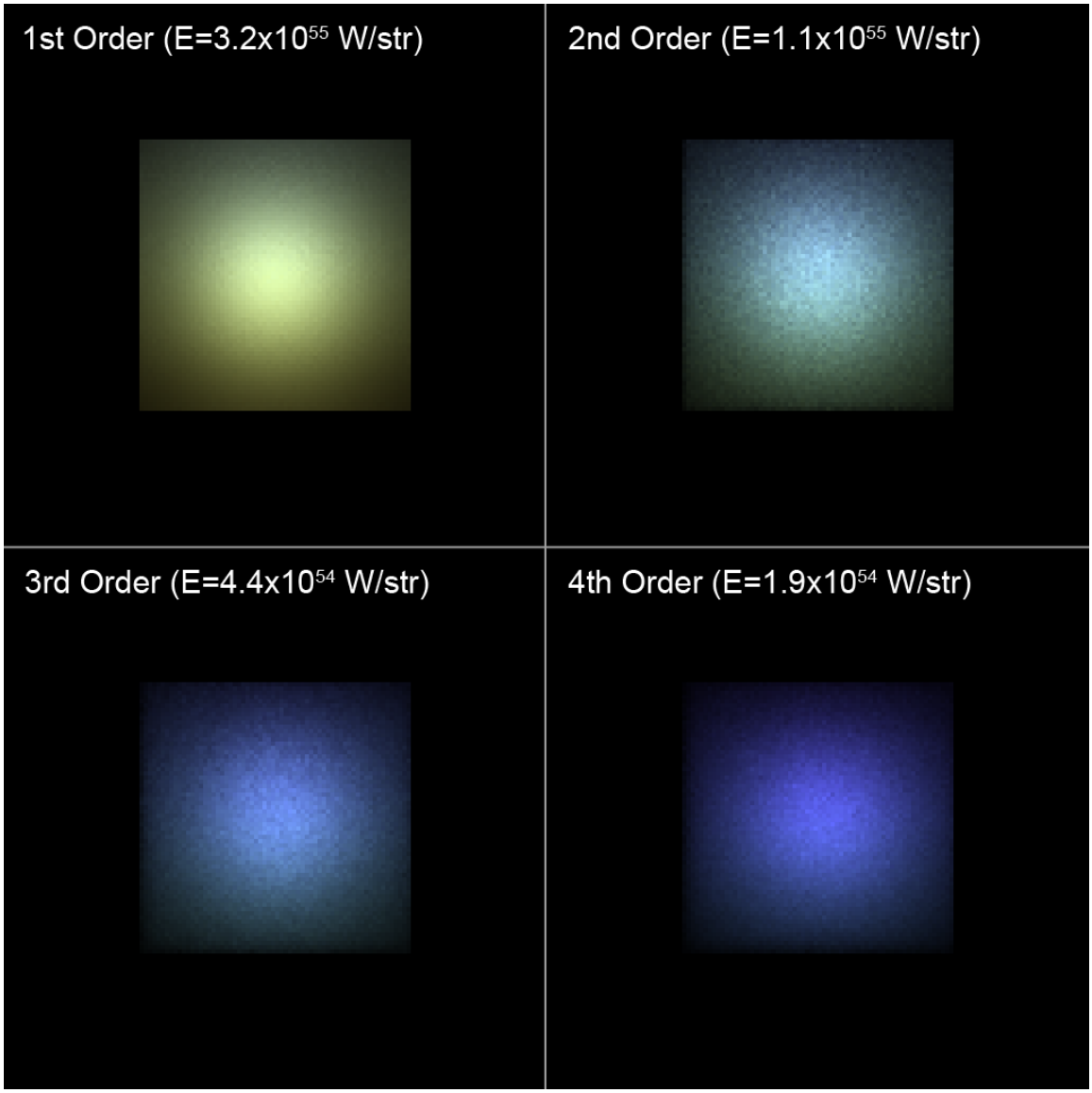

Figure 0-4: Results of multiple scattering in SHAPE. The results were generated using the same example as for single scattering. Each panel represents the image formed by successively increasing orders of scattering. The images *do not* include contributions from the previous order. As the number of iterations increases, the scattered emission gets reduced in intensity and shifted to shorter wavelengths. As well, the central bright region becomes dispersed.

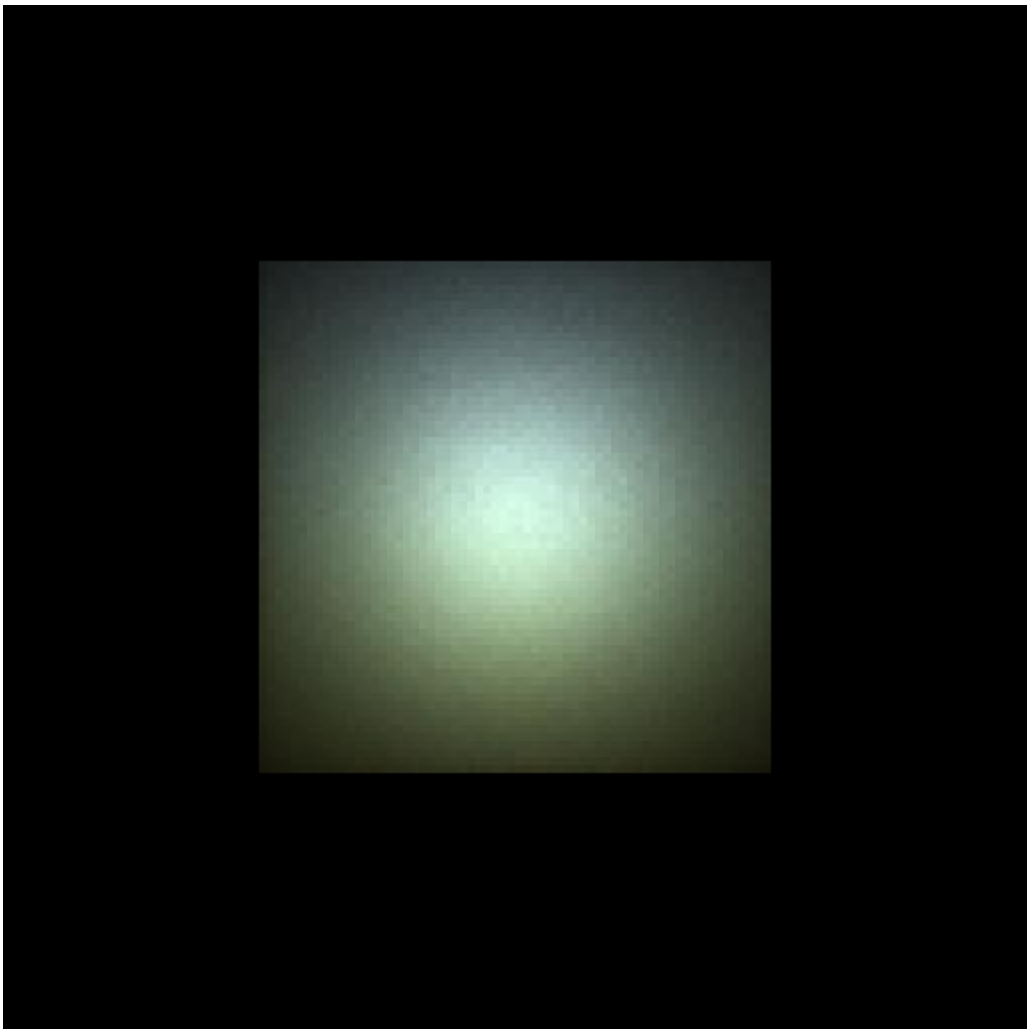

Figure 0-5: SHAPE image representing the combination of four iterations ($m = 4$) of scattering (combination of all images in Figure 0-4). The color and structure of the image is very similar to the single scattering case (top left panel of Figure 0-4) indicating the small qualitative effect of multiple scattering on this particular model.

1.5 Dust

The equations of radiative transfer require the input of emission, absorption and scattering coefficients for each frequency, ν. The calculation of these coefficients depends on local conditions in each cell of the grid, such as density and temperature. The physics module in SHAPE allows for the creation of "species" which govern how the coefficients are calculated. When the grid is created, SHAPE determines which species belong to which cells and the cell conditions are used to create the coefficients.

The species used most extensively throughout this thesis is dust. In order to realistically reproduce the absorption and scattering by dust, accurate coefficients must be calculated. For a spherical dust grain of radius a and incident light of wavelength λ, we define the parameter:

$$x(a) = \frac{2\pi a}{\lambda} \tag{1.48}$$

The extinction coefficient (absorption coefficient + scattering coefficient) of the grain is:

$$\kappa_\nu = \pi a^2 Q_\nu(x) n_d(a) \tag{1.49}$$

Where n_d is the number density of the dust and $Q_\nu(x)$ is the extinction efficiency (normalized extinction cross section). The extinction efficiency is composed of an absorption (a) and scattering(s) component:

$$Q_\nu(x) = Q_\nu^a(x) + Q_\nu^s(x) \tag{1.50}$$

Which then yields expressions for the absorption and scattering coefficients:

$$\kappa_\nu^a = \pi a^2 Q_\nu^a(x) n_d(a) \tag{1.51}$$

$$\kappa_\nu^s = \pi a^2 Q_\nu^s(x) n_d(a) \tag{1.52}$$

The extinction efficiency can be calculated by invoking Mie Theory; an analytic solution of Maxwell's equations developed by Gustav Mie for the scattering of light off spherical particles (Mie 1908). In order to perform this calculation, the complex index of refraction for the dust grain is required:

$$m = n - ik \tag{1.53}$$

n is the refractive index, k is the absorption index and both are referred to as the optical constants. Calculating absorption coefficients via Mie theory is quite involved and computationally expensive so several approximations have been developed. For very small grains ($x \ll 1$), the extinction efficiencies are given by:

$$\boxed{Q_\nu^a(x) \simeq \frac{8}{3} x^4 \left| \frac{m^2 - 1}{m^2 + 2} \right|^2} \tag{1.54}$$

$$\boxed{Q_\nu^s(x) \simeq -4x \mathrm{IM}\left(\frac{m^2 - 1}{m^2 + 2} \right)} \tag{1.55}$$

For very large grains ($x \gg 1$) $Q_\nu(x) = 2$ via Babinet's theorem (see e.g. Krugel 2008). However, this does not give any specific information about the values of $Q_\nu^a(x)$ and $Q_\nu^s(x)$. If the grain does not absorb (i.e. $k \sim 0$) trivially $Q_\nu^a(x) = 0$ and $Q_\nu^s(x) = 2$. When $k > 0$ we can estimate the absorption coefficient by using the reflectance of the grain. The reflectance of a plane surface is the fraction of incident light that is reflected (Krugel 2008):

$$r = \left| \frac{1 - m}{1 + m} \right|^2 \tag{1.56}$$

Assuming, for simplicity, the light is hitting the grain at an angle normal to its surface, we can calculate the reflection efficiency as:

$$\pi a^2 Q^{\text{ref}} = r \tag{1.57}$$

The absorption efficiency is related to the reflection efficiency as:

$$Q^a = 1 - Q^{\text{ref}} \tag{1.58}$$

Therefore our absorption efficiency in the large grain approximation is:

$$\boxed{Q_\nu^a(x) \simeq 1 - \left|\frac{1-m}{1+m}\right|^2} \tag{1.59}$$

And our scattering efficiency is:

$$\boxed{Q_\nu^s(x) \simeq 2 - Q_\nu^a(x) = 1 + \left|\frac{1-m}{1+m}\right|^2} \tag{1.60}$$

Dust grains come in a variety of sizes, and each size contributes to a different part of the spectrum. Large grains tend to influence the infrared, whereas smaller grains affect the optical and UV (Krugel 2003). It is thus necessary to include grains over a range of sizes to accurately reproduce dust properties. Mathis, Rumpl and Nordsieck 1977 found a power law size distribution that closely fit the observed interstellar reddening curve. The power law:

$$n_d(a) \propto a^{-q} \tag{1.61}$$

was best fit with an exponent of $q = 3.5$. This so-called MRN size distribution is integrated with a minimum ($a_{\min}$) and maximum ($a_{\max}$) grain size to calculate the absorption and scattering coefficients:

$$\kappa_\nu^a = \int_{a_{\min}}^{a_{\max}} \pi a^2 Q_\nu^a(x(a)) \beta a^{-q} da \tag{1.62}$$

$$\kappa_\nu^s = \int_{a_{\min}}^{a_{\max}} \pi a^2 Q_\nu^s(x(a)) \beta a^{-q} da \tag{1.63}$$

Where β is a normalization parameter found by requiring:

$$n_d = \int_{a_{\min}}^{a_{\max}} n_d(a) da = \int_{a_{\min}}^{a_{\max}} \beta a^{-q} da \tag{1.64}$$

In SHAPE, equations (1.62) and (1.63) are solved for a given set of parameters, $a_{\min}, a_{\max}, q, n, k$. The n, k variables are functions of frequency and can be entered via an analytic function or discreet points for each spectral band in the beam. SHAPE has several "preset" dust species: amorphous carbon, silicate and graphite. For each of these sub-species, the n and k coefficients are automatically set to the values given by Krugel 2008 in his figures 5.10, 5.11 and 5.12.

The above derivation assumes that the grains are either very large or very small with respect to the wavelength of the incident light. When the wavelength of the light and the radius of the grain are approximately equal, a full Mie calculation must be implemented. SHAPE is capable of the exact Mie calculation, but it is time consuming and the approximations described above are preferred whenever possible. The Mie code implemented in SHAPE is a transcription of the FORTRAN code by N.V. Voshchinnikov (Voshchinnikov 2002) into JAVA.

The smallest wavelength rendered in this thesis is $\sim 4 \times 10^{-7}\,\mathrm{m}$. The dust radii used range from $\sim 1 \times 10^{-9}\,\mathrm{m}$ in graphites to $\sim 2 \times 10^{-7}\,\mathrm{m}$ in amorphous carbon and silicates. Graphs showing the approximate solution (equations (1.54) and (1.55)) and the full Mie solution for the absorption, scattering and extinction efficiencies are given in Figure 0-6. The approximate and full Mie

solutions diverge around $a = 5\times10^{-8}\,\mathrm{m}$. If we integrate the MRN function, equation (1.61), over our range of grain sizes, we have:

$$n_{\text{total}} = \int_{a_{\min}}^{a_{\max}} \beta a^{-q} da = \beta \left[\frac{a^{1-q}}{1-q} \right]_{a_{\min}}^{a_{\max}} \tag{1.65}$$

Where β is a constant found through normalization. For $q = -3.5$, $a_{\min} = 2\times10^{-8}\,\mathrm{m}$ and $a_{\max} = 2\times10^{-7}\,\mathrm{m}$ we get $n_{\text{total}} = \beta \cdot 7.05\times10^{18}\ \mathrm{m^{-3}}$. The density of dust with sizes greater than the divergence at $a_{\text{div}} = 5\times10^{-8}\,\mathrm{m}$ is $n_{\text{total}} = \beta \cdot 6.93\times10^{17}\ \mathrm{m^{-3}}$. The number of grains that make up sizes greater than the divergence is therefore $\sim 9\%$. The large majority of grain sizes used in this thesis is consequently adequate for the Mie approximation.

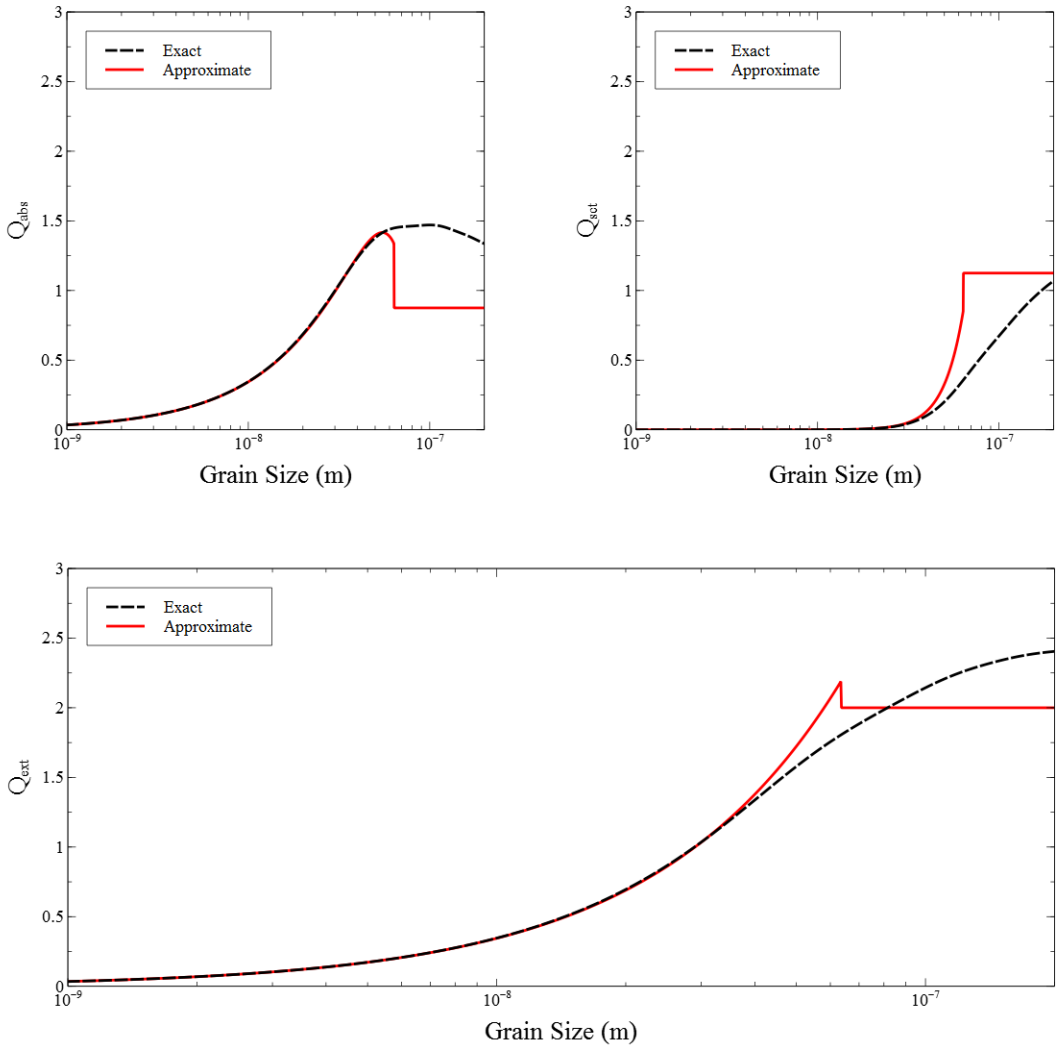

Figure 0-6: A comparison between the exact and approximate Mie solutions to the absorption efficiency (Q_{abs}), scattering efficiency (Q_{sct}) and extinction efficiency (Q_{ext}) for grain sizes between $a = 1\times10^{-9}\,\text{m}$ and $a = 2\times10^{-7}\,\text{m}$. The calculations use a wavelength of $4\times10^{-7}\,\text{m}$. Near $a = 5\times10^{-8}\,\text{m}$ the exact and approximate solutions begin to diverge and the small grain approximation is no longer valid.

1.6 Ionization

Ionization occurs when a photon of sufficient energy causes an electron to be ejected from an atom. Recombination with ejected electrons by ionized atoms then leads to line emission. The central star of a PPN is not hot enough to supply photons of adequate energy to ionize hydrogen and we therefore see no line emission from ionized atoms in PPNs. However, as the star increases in temperature the nebula begins to ionize and the PPN becomes a PN.

To study this transition from PPN to PN, we must be able to simulate scattering and ionization. The ionization structure of the nebula is supported by the UV output from the central star. At each point in an ionized nebula, the recombination rate to each level in the H atom is equal to the ionization rate from the ground state of H atom. The total number of ionizing photons emitted by a star of temperature T_* and radius R_* is:

$$Q = \int_{\nu_1}^{\infty} \frac{4\pi {R_*}^2 \pi B_\nu(T_*)}{h\nu} d\nu \tag{1.66}$$

Where ν_1 is the minimum frequency required to ionize a photon from the ground state of H (called the Lyman limit), and where $B_\nu(T_*)$ is the Planck function:

$$B_\nu = \frac{2h\nu^3}{c^2} \frac{1}{e^{h\nu/kT} - 1} \tag{1.67}$$

The total number of recombinations in the ionized volume is:

$$\Re = \int n_p n_e \alpha_B dV \tag{1.68}$$

Where n_p, n_e, α_B are the number density of protons, number density of electrons and total recombination coefficient respectively. By integrating (1.66) and (1.68) for a spherical nebula and equating the results, we can solve for the radius of the ionized portion of the nebula:

$$r_s = \left[\frac{45 G(T_*) L_*}{4\pi^5 k T_* n_H^2 \alpha_B(T_e)} \right]^{1/3} \tag{1.69}$$

Where L_* is the luminosity of the star, n_H is the number density of hydrogen and:

$$G(T_*) = \int_{\frac{h\nu_1}{kT_*}}^{\infty} \frac{x^2}{e^x - 1} dx \tag{1.70}$$

Equation (1.69) is the so-called Strömgren radius (see Kwok 2007 for full derivation) and represents the size of the ionized region for a 1D spherical nebula.

Almost all PNs are aspherical and therefore (1.69) is inadequate to determine the ionized region(s) of the nebulae. The approach taken by SHAPE is to determine locally, per cell, whether ionization can be sustained. If the number of ionizing photons is greater than the number of recombinations within a cell, that cell is considered ionized. The algorithm is as follows:

A beam of n spectral bands is first cast from the source to the cell in question. Radiative transfer is performed on the beam along the path travelled. The number of photons with energies above the Lyman limit are then counted and this becomes the number of ionizing photons for the cell Q_{cell}.

To determine the number of recombinations per cell, we use equation (1.68) over the volume of the cell to get:

$$\Re_{\text{cell}} = n_p n_e \alpha_B V_{cell} \tag{1.71}$$

In an ionized hydrogen nebula, we assume that $n_p = n_e = n_H$. The total recombination coefficient is supplied by the user, and has a default value of $2.59 \times 10^{-19} \text{m}^3\ \text{s}^{-1}$ at $T_e = 1 \times 10^4\ \text{K}$. If the number of ionizing photons reaching the cell is greater than the number of recombinations ($Q_{\text{cell}} \geq \Re_{\text{cell}}$), the cell is said to be ionized and the H within the cell will be set to emit.

Figure 0-7 shows the theoretical and SHAPE Strömgren radius as a function of star temperature, T_* (ranging from $1 \times 10^4 - 7 \times 10^4\ \text{K}$) for a constant stellar luminosity of $L_* = 10^4 L_\odot$. The Strömgren radius for three different nebular densities is plotted. The SHAPE radii very closely match the theoretical radii. The advantage of SHAPE, however, is that the same algorithm can be applied to a 3D environment and therefore the ionization structure of aspherical PNs can be determined. Furthermore, the transition from the pure scattering of PPNs to the ionized nebulae of PNs can be studied.

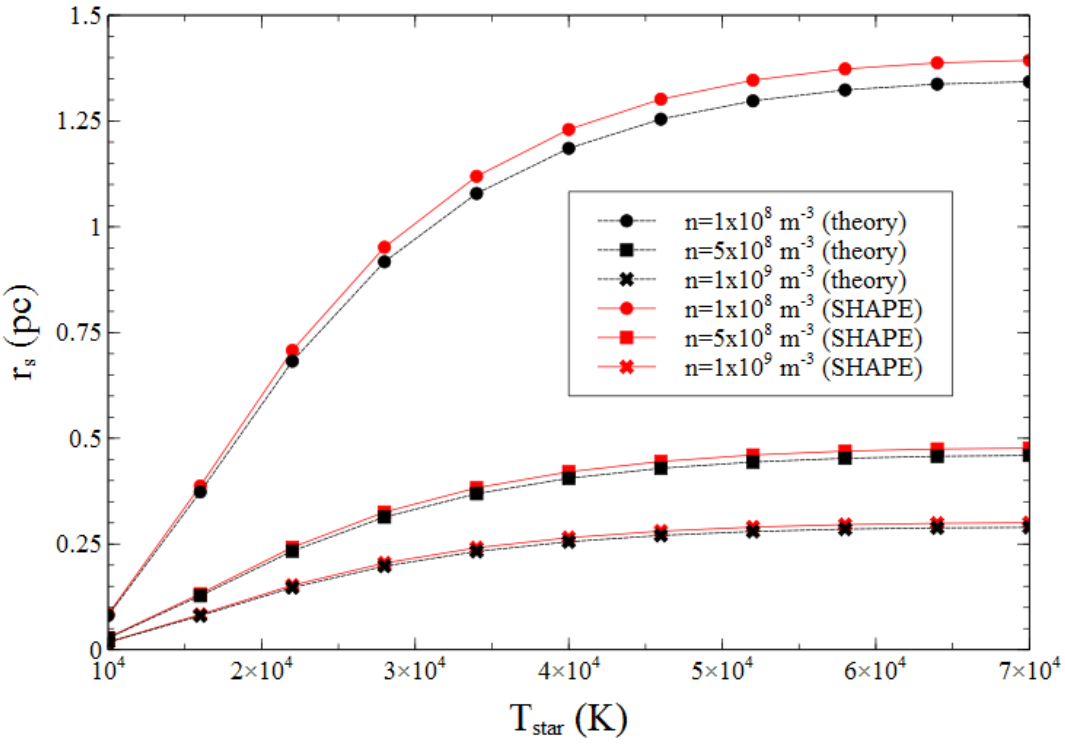

Figure 0-7: A comparison between the Strömgren radius vs. T_* calculated from equation (1.69) (black dotted line) and calculated using SHAPE (red solid line) for three different nebular densities. The central star maintains a luminosity of $L_* = 10^4 L_\odot$ throughout the simulation.

References

Krugel, E 2003, *The Physics of Interstellar Dust*, Institute of Physics Publishing.

Krugel, E 2008, *An Introduction to the Physics of Interstellar Dust*, Taylor & Francis Group.

Kwok, S 2007, *Physics and Chemistry of the Interstellar Medium*, University Science Books.

Mathis, JS, Rumpl, W & Nordsieck, KH 1977, 'The size distribution of interstellar grains', *Astrophysical Journal*, vol 217, pp. 425-433.

Mie, G 1908, 'Beiträge zur Optik trüber Medien, speziell kolloidaler Metallösungen', *Annalen der Physik*, vol 330, no. 3, pp. 377-445.

Voshchinnikov, NV 2002, *Light scattering software*, viewed 14 June 2011, <http://www.astro.spbu.ru/staff/ilin2/DOP/6-SOFT/ours.html>.